euspen's 25th International Conference & Exhibition, Zaragoza, ES, June 2025
www.euspen.eu

Orthogonal cutting of polymer for the validation of material models

Henning Specketer[1], Wei Wang[2], Oltmann Riemer[2,3], Kai Rickens[2] and Bernhard Karpuschewski[2,3]

[1] *Faculty for Production Engineering, University of Bremen, Germany*

[2] *Laboratory for Precision Machining LFM, Leibniz Institute for Materials Engineering IWT, Germany*

[3] *MAPEX Center for Materials and Processes, University of Bremen, Germany*

riemer@iwt.uni-bremen.de

Abstract

The finite element method (FEM) has proven to be an effective approach for numerically solving differential equations in engineering and mathematical modeling. Constitutive models employed in manufacturing processes and FEM simulations are pivotal for understanding and optimizing attributes such as surface roughness, residual stresses, micro-hardness, plastic deformation, phase transitions, elastic recovery, ball indentation, and thermal behaviour. While FEM has been extensively applied to the cutting processes of metallic materials—most commonly utilizing the Johnson-Cook material model—the adaptation of such techniques to polymers remains relatively unexplored. The significant differences in material behaviour between metals and polymers present challenges in directly modifying metal-based FEM models for polymeric materials.
This study focuses on advancing the understanding of polymer material behaviour through orthogonal cutting experiments conducted on Polymethyl methacrylate (PMMA). Experiments were performed across varying cutting depth (a_p) and cutting speed (v_c), with analyses focused on their influence on key metrics, including cutting force (F_c), thrust force (F_p), and chip geometry. These findings aim to inform the development and validation of FEM simulations tailored to polymer cutting conditions. Future work will incorporate FEM simulations under the same cutting parameters to validate and refine the models presented in this study, with potential applications in precision machining of polymers, such as intraocular lens (IOL) manufacturing.

Polymer; Diamond Turning; Material model; Orthogonal cutting; Ultra-Precision

1. Introduction

The finite element method (FEM) has emerged as a powerful tool for advancing manufacturing technologies by enabling the simulation and analysis of key metrics, such as surface roughness, residual stresses, cutting forces, and thermal behaviour [1]. Despite its extensive application in metal machining, the use of FEM for polymers remains limited due to the availability and complexity of material models. The substantial differences in material behaviour between metals and polymers pose significant challenges in adapting metal-based FEM models to accurately represent polymeric materials. However, such advancements could be instrumental in improving the precision machining of polymer products, such as intraocular lenses (IOLs).

IOLs are critical optical devices surgically implanted to replace the natural crystalline lens in cataract patients, which is the only effective method to treat cataract [2]. The global IOL market is valued at an estimated USD 4.6 billion in 2023 and is anticipated to expand to USD 6.8 billion by 2030, reflecting a compound annual growth rate (CAGR) of 5.7% over the forecast period (2023–2030) [3]. Different from standard IOL—fabricated by moulding processes, customized lenses are fabricated using diamond turning, enabling precise correction of individual aberrations for improved visual outcomes [4,5]. The demand for a FEM of polymer arises when optimizing machining parameters for the customized IOL production, particularly for those with difficult-to-machine materials, such as hydrophobic polymers with low glass transfer temperature (T_g) as they exhibit significant variations in mechanical behavior across different temperature ranges [6,7].

This study investigates polymethyl methacrylate (PMMA) as an initial material for developing a FEM of polymer cutting. PMMA is widely used in IOLs due to its biocompatibility, longevity, mechanical properties and good optical performance [2]. The aim of this work is to create a referenceable database that will enable future FEM models to validate their theoretical validity by comparing them with real measurement data.

In previous research work, Richeton et al. [8] model the influences of strain rate (from 0.0001 1/s to 5000 1/s) and temperature (from -100 °C to 120 °C) on the stress-strain curves of PMMA and validate their results through compression tests. Similarly, Abdel-wahab et al. [9] study the temperature-dependent mechanical behaviour of PMMA with FEM and validate their findings through tensile and three-point bending test. Similarly, existing FEM material models, such as the work of M. Nasraoui et al. [10] and J. Qiu et al. [11], focus on the simulation of such stress-strain curves, which are usually obtained from tensile or compression tests.

In order to extend the application range of future models, there is a need for additional data sets that focus specifically on the prediction of acting forces and chip formation in processes such as diamond turning. This work should therefore contribute to the development of a more comprehensive understanding of the material-dependent process parameters and create a basis for more precise FEM simulations.

2. Experiment Design

The focus of the evaluation is on the average cutting and thrust forces due to the test and with regard to the validation of possible FEM models, as the feed force does not play a significant role in a grooving or planing test.

The test setup was designed to replicate the conditions of an orthogonal cutting process as precisely as possible. These framework conditions had a significant influence on the choice of tool and the design of the specimen. A schematic representation of the sample design can be found in Figure 1.

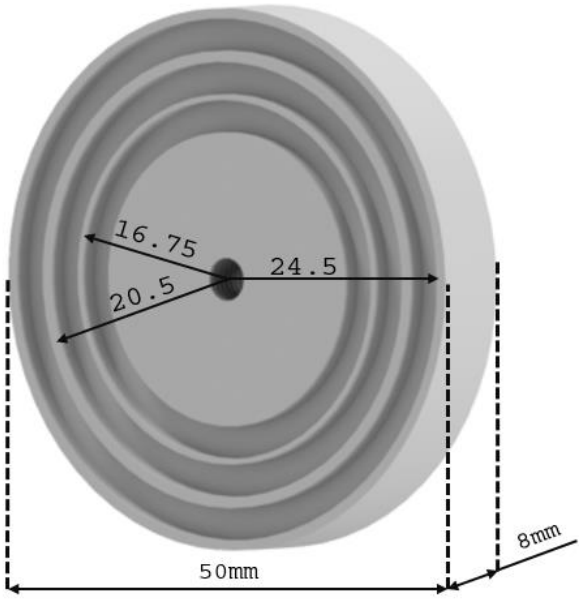

Figure 1. Design of the PMMA sample used in the orthogonal cutting experiments. The sample features three tubular ridges with widths of 1 and 0.5 mm.

The sample material has a diameter of 50 mm and exhibits three tubular ridges with rectangular cross section. The two outer ridges have a width of 1 mm each and the inner ridge with a width of 0.5 mm. The gaps between the ridges were designed to ensure free cutting. A maximum cutting depth of 2 mm is available for the orthogonal plunge cutting experiments with axial feed direction, which ensures multiple machining passes and the structural stability of the ridges.

The diamond cutting tool (Contour Fine Tooling BV, Valkenswaard, Netherland) has a trapezoidal geometry with a straight cutting edge, as shown in Figure 2. The width of the cutting edge is 2895 µm, the rake angle is 0° and the clearance angle is 5°.

This straight cutting edge ensures the machining of the entire ridges and enables an even distribution of the cutting forces and a constant cutting depth, ensuring scalable force data set.

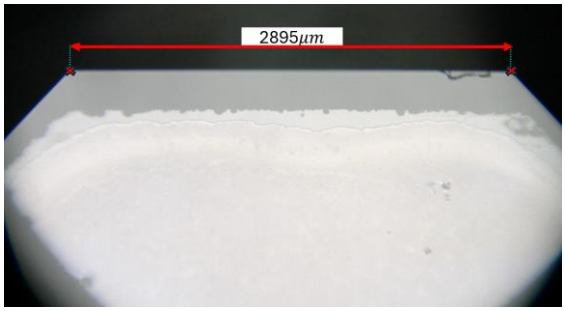

Figure 2. Trapezoidal diamond tool with straight cutting edge.

The samples were machined on a Nanotech 500 FG (Moore Nanotechnology Systems LLC, Swanzey, United States), a high-precision diamond lathe. A piezoelectric dynamometer MiniDyn, Kistler type 9119AA1 (Kistler Instrumente AG, Wintherthur, Switzerland) was used to record the cutting forces at a sampling frequency of 10 kHz. A camera system was used to actively monitor the machining process. The entire test setup can be seen in Figure 3.

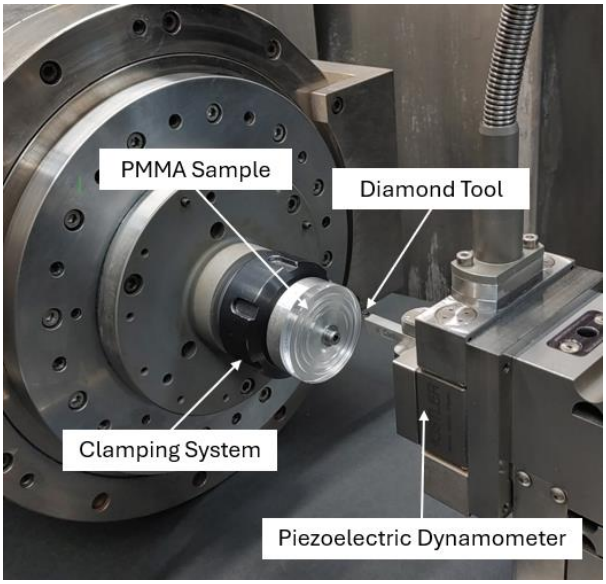

Figure 3. Test setup for machining experiments.

Test machining series focussed on varying parameters such as cutting depth, rotational speed and cutting speed, which is dependent on the radius. In addition, the axial infeed is investigated, which in this orthogonal cutting kinematic is equivalent to the uncut chip thickness per revolution. The evaluation is based on the averaged cutting and thrust forces as well as the analysis of the resulting chip thickness. The distribution and direction of the forces are shown in Figure 4. In summary, the setup includes a PMMA sample securely clamped in a high-precision clamping system, the diamond tool positioned for cutting, and the instrumentation used to record the forces.

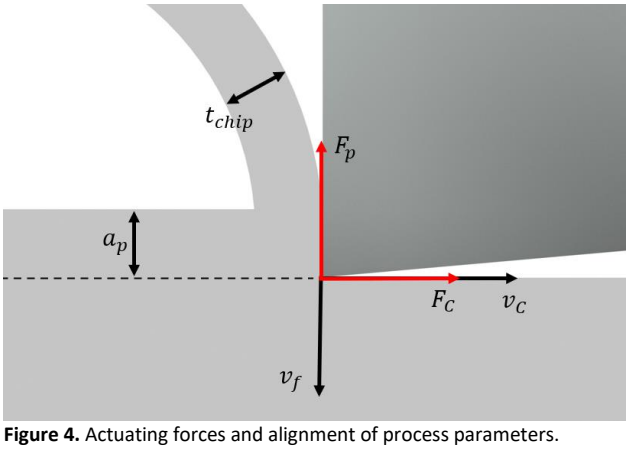

Figure 4. Actuating forces and alignment of process parameters.

The design of experiments aimed at the broadest possible data basis for force measurements that correlate with the cutting speed. In advance of the cutting experiments the entire sample was face turned with a depth of cut of 0.1mm to ensure accurate alignment. The ridges were then machined iteratively to a total depth of 0.5 mm per pass.

The rotational speed was adjusted to keep the cutting speed constant over the changing radii. In addition, the cutting depth per revolution was varied, with the control range being between 10 and 20 µm per revolution. The influence of a cutting depth of 40 µm on the forces was also investigated in two separate machining runs. Table 1 provides an overview of the experimental configuration.

Table 1. Experimental configuration.

Parameter	Values
Turning speed *n* [1/min]	100, 120, 500, 598, 1000
Feed Speed v_f $[mm/min]$	1, 2, 10, 12, 20, 40
Cutting depth a_p $[\mu m]$	10, 20, 40

3. Results

All three cutting forces, i.e. feed force, cutting force and thrust force were recorded during the cutting processes. The recorded raw force data was processed and analysed using the in-house MesUSoft 3 software. Figure 5 shows exemplary cutting and thrust forces reduced by a factor 8 to 1250 Hz, for a cutting speed of v_c of 257 mm/s, depth of 20 μm during turning a 1 mm ridge.

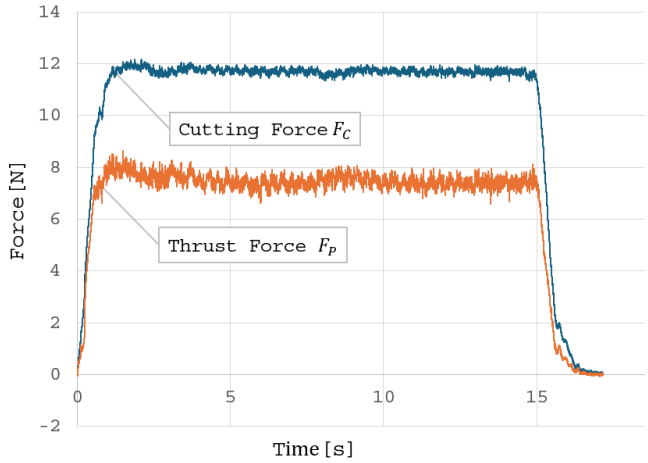

Figure 5. Measured cutting and thrust forces of PMMA at a turning speed *n* of 100 round per minute.

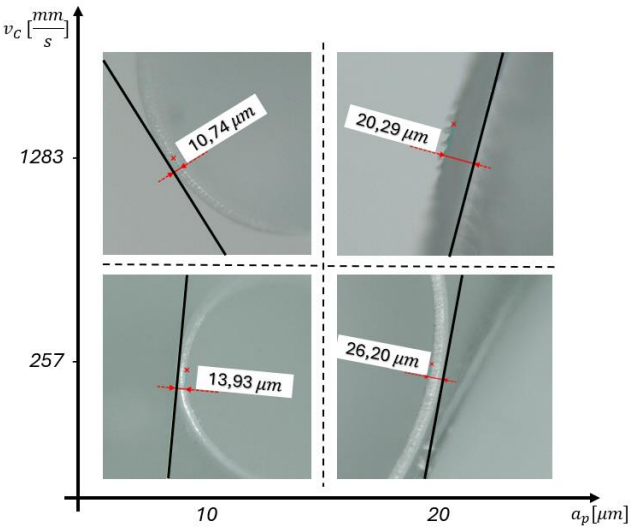

Figure 6. Compares the chip thickness in relation of cutting speed v_c and cutting depth a_p.

Chips were collected during each experiment to determine the average chip thickness. The examination and measurement were conducted using a Keyence VHX-6000 digital microscope (Keyence GmbH, Neu-Isenburg, Germany). The analyses were performed with VH-Z100R objective lens, utilizing magnifications of 400x and 900x to ensure precise characterization of the chips. Figure 6 shows typical chip analyses for four different machining conditions.

The machining conditions and results of the test series are summarized in Table 2. The data was sorted according to the ascending cutting force and cutting depth. It can be seen that the cutting speed has no significant influence on the acting cutting forces. However, it is noticeable that the thrust force deviates from this trend. This is due to the increased feed rate, which is inevitably caused by the increase in rotational speed.

Table 2. Machining conditions and results of the test series.

v_c [mm/s]	a_p [µm]	n [1/min]	w_{ridge} [mm]	F_C [N]	F_P [N]	t_{chip} [µm]
175	10	100	0.5	2.9	2.1	13.8
175	20	100	0.5	5.7	4.4	20.3
175	40	100	0.5	9.7	5.2	46.9
175	40	100	1	14.6	9.5	45.2
215	20	100	1	9.7	6.6	23.0
215	20	100	1	10.3	6.6	25.2
257	10	100	1	5.6	3.9	13.5
257	10	100	1	5.8	3.9	13.5
257	20	100	1	9.2	6.8	22.3
257	20	100	1	10.6	6.4	24.2
257	10	120	1	4.7	3.2	11.2
257	20	120	1	7.7	3.5	15.8
1283	10	500	1	4.9	2.0	12.9
1283	20	598	1	8.7	2.9	18.7
1754	10	1000	0.5	2.5	0.9	11.5
1754	20	1000	0.5	4.6	1.6	21.2
2147	10	1000	1	5.0	1.5	11.4
2147	20	1000	1	8.0	2.2	18.3
2566	10	1000	1	5.0	1.4	11.4
2566	20	1000	1	7.3	2.0	18.7

Another notable effect is the compression of material in the contact zone, which is clearly evident from the measured chip thicknesses. For example, although the nominal cutting depth is 20 µm, the average chip thickness is 21 µm. This indicates that the chip is thicker than the set depth of cut, which is typical of plastic deformation and chip compression in the cutting zone. In addition, the results indicate that the chip thickness decreases with increasing cutting speed.

However, it should be noted that the measured chip thicknesses are for guidance only. Due to the continuous chip shape and the resulting curling of the chips, it was not possible to guarantee a consistently precise vertical view in all cases.

Figure 7 shows the correlation of cutting and thrust force (F_c and F_p) depending on turning speed n. Assuming linear dependency, it can be seen that both, cutting and the thrust force, significantly decrease with increasing rotational speed. Similar phenomena has also been observed in the work of Wang et al. [6], where both PMMA and hydrophobic polymer SHi49 blanks are face-turned at different beginning temperature. It should be emphasized that the thrust force is reduced proportionally faster than the cutting force. Which can be explained by the cutting mechanics, e.g. friction and shearing.

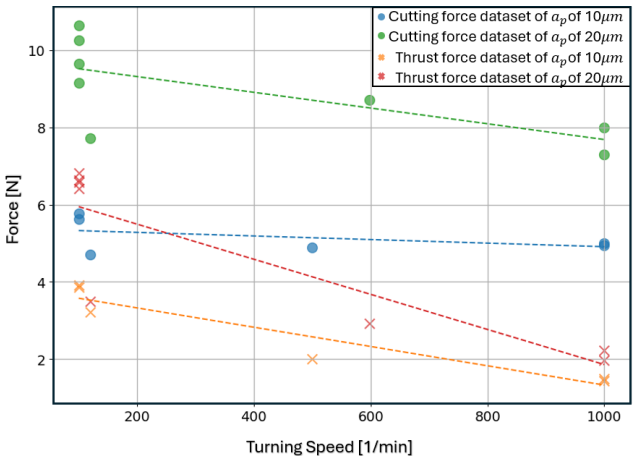

Figure 7. Cutting F_C and thrust force F_P over turning speed n for orthogonal machining at cutting depths of $a_p = 10$ or $20\mu m$.

Firstly, an increase in rotational speed leads to increased friction in the shear zone, which causes a local increase in temperature. This temperature increase contributes to material softening, which reduces the material resistance. Secondly, the rotational speed influences chip formation. As can be seen in Figure 6, the material moves faster through the shear zone at higher speeds. This reduces the proportion of plastic deformation work, as less time is available for the complete plastic deformation of the material.

4. Summary and future work

A series of orthogonal cutting tests was carried out to achieve a well-founded assessment of the material behaviour of PMMA during turning.

- First of all, it can be seen that the influence of the cutting and rotational speed (v_C and n) on the cutting force F_C is comparatively low, but decreases with increasing rotational speed n. In contrast, the thrust force F_P is much more strongly influenced by this effect.

- In addition, the effect of material compression in front of the contact zone can be mapped by evaluating the chip thickness t_{chip}. As the cutting speed v_C increases, this effect is reduced, resulting in thinner chips.

- Based on these findings, conclusions can be drawn about the scalability of the acting forces. A comparison of identical ridge widths with varying cutting depths shows an almost linear scaling between the increase in cutting depth and the increase in the acting forces.

The knowledge gained from this research enables to validate FEM models for the diamond turning of PMMA. With the help of scaling factors, both two-dimensional models and comparisons with three-dimensional models under similar boundary conditions can be used. The generation of further data sets is of paramount importance for future investigations. In particular, the influence of the tool geometry and the variation of the cutting depth are relevant factors. In addition, the effect of different ambient temperatures should be taken into account, as these significantly influence the elasto-plastic material behaviour of polymers, especially those with low T_g, such as hydrophobic ones.

Acknowledgements

The idea for this paper was inspired by work conducted in Project “Efficient and flexible production of hydrophobic free-form surfaces of intraocular lenses by fast-tool servo diamond turning”, which is funded by the German Federal Ministry of Education and Research (BMBF) within the “SME-innovative: Production Research” funding measure (funding number 02P21K521) and managed by the Project Management Agency Karlsruhe (PTKA). The authors would like to express their gratitude to Dr. Lars Langenhorst (Leibniz Institute for Materials Engineering IWT, Germany) for his constructive advice and numerous contributions during the work.

References

[1] Quiza, R.; López-Armas, O.; Davim, J.P. Finite Element in Manufacturing Processes. 2012; 13-37

[2] Yu, N.; Fang, F.; Wu, B.; Zeng, L.; Cheng, Y. State of the art of intraocular lens manufacturing. The International Journal of Advanced Manufacturing Technology 2018, 98, 1103-1130

[3] Global Industry Analysts, I. Intraocular Lenses - Global Strategic Business Report; 2024; 266

[4] Schrecker, J.; Schröder, S.; Langenbucher, A.; Seitz, B.; Eppig, T. Individually Customized IOL Versus Standard Spherical Aberration-Correcting IOL. J Refract Surg 2019, 35, 565-574

[5] Schröder, S.; Eppig, T.; Liu, W.; Schrecker, J.; Langenbucher, A. Keratoconic eyes with stable corneal tomography could benefit more from custom intraocular lens design than normal eyes. Scientific Reports 2019, 9, 3479

[6] Wang, W.; Riemer, O.; Rickens, K.; Eppig, T.; Karpuschewski, B. Machinability of hydrophobic acrylic polymer for customized intraocular lenses. In Proceedings of the The 9th International Conference on Nanomanufacturing (nanoMan2024), Concorde Hotel Singapore, 01-04 December 2024, 2024; 100-103

[7] Wang, W.; Riemer, O.; Rickens, K.; Eppig, T.; Karpuschewski, B. Off-Axis Fast-tool-servo diamond turning of customized intraocular lenses from hydrophobic acrylic polymer. In Proceedings of the euspen's 24th International Conference & Exhibition, University College Dublin, Dublin, IE, 10-14 June 2024, 2024; 221-222

[8] Richeton, J.; Ahzi, S.; Vecchio, K.S.; Jiang, F.C.; Makradi, A. Modeling and validation of the large deformation inelastic response of amorphous polymers over a wide range of temperatures and strain rates. International Journal of Solids and Structures 2007, 44, 7938-7954

[9] Abdel-Wahab, A.A.; Ataya, S.; Silberschmidt, V.V. Temperature-dependent mechanical behaviour of PMMA: Experimental analysis and modelling. Polymer Testing 2017, 58, 86-95

[10] Nasraoui, M.; Forquin, P.; Siad, L.; Rusinek, A. Influence of strain rate, temperature and adiabatic heating on the mechanical behaviour of poly-methyl-methacrylate: Experimental and modelling analyses. Materials & Design 2012, 37, 500-509

[11] Qiu, J.; Jin, T.; Su, B.; Duan, Q.; Shu, X.; Liu, E.; Li, Z. Strain Rate Sensitivity of Yield Response of PMMA: Experimental Characterization and Material Modeling. Journal of Testing and Evaluation 2020, 48, 3752-3767